

Active Defects Generated in Silicon by Laser Doping Process

A. Barhdadi^{1,*}, B. Hartiti² and J-C. Muller³

¹*Physics of Semiconductors and Solar Energy Laboratory, Ecole Normale Supérieure,
University Mohammed V-Agdal, Takaddoum, Rabat, Morocco*
and

The Abdus Salam International Centre for Theoretical Physics, Trieste, Italy

²*Laboratory of Materials Physics and Applications of Renewable Energy, Faculté des Sciences et Techniques,
University Hassan II, Mohammedia, Morocco*

³*Institut d'Electronique du Solide et des Systèmes, CNRS, Strasbourg, France*

Schottky diodes have been made on both n-type and p-type virgin mono-crystalline silicon processed by three kinds of pulsed lasers currently used in new photovoltaic technologies. The electrical characteristics of these diodes have been measured as a function of laser fluence. A strong change in all of their electrical parameters occurs for fluence equal or higher than a threshold at which the processed silicon surface layer turns into melt. Capacitance versus voltage measurements and DLTS analyses show that laser irradiations introduce a large density of deep levels related to active defects in the processed surface and bulk area. These defects are believed mostly generated during the fast quenching rate in pulsed laser treatments.

1. Introduction

In the fabrication of solar cells, dopant diffusion process is required to form junctions. Recently, instead of the conventional impurity diffusion method at high temperatures, laser doping technique [1] has been noticed as a promising alternative process because of its several advantages [2,3]. This technique is based on processing semiconductors by means of focused laser beam. It can be performed at room temperature, which is leading to the reduction of thermal stress in the substrate. This improves the cell fabrication yield especially in the case of thinner silicon substrate (below 150 μm). In addition, the selective diffused area for emitter or BSF can be easily formed without using the conventional photolithography process. This has the added advantage of not disemboque wastes.

In fact, processing semiconductors, using focused laser radiation, has already been known for more than 30 years. A first phase of strong research interest spanned the late 1970s and the 1980s, with a tremendous number of publications establishing a theoretical and experimental base for the understanding of the process. White et al. [4-6] and Wood et al. [7-9] were among the key researchers on this topic. A fine compilation of most results is found in [10] or [11]. The majority of these fundamental experiments was conducted with ion-

implanted silicon layers, which were annealed by laser irradiation. Thus, the experiments were not about 'real' laser doping. Nevertheless, they produced a number of valuable findings such as: (a) laser melting of the silicon surface leads to an epitaxial re-growth of the silicon on the underlying substrate; (b) the implanted impurity atoms are incorporated into substitution lattice sites during the re-crystallization and their concentrations C_L are significantly exceeding the equilibrium solubility limit C_0 , as well as their segregation coefficients k_L , which are also exceeding the equilibrium values k_0 ; (c) the values of C_L and k_L are depending on the re-crystallization velocities V_{cryst} , which are in the range of several m.s^{-1} .

At the same time, following the fundamental research, a number of authors reported results from 'real' laser doping experiments using different types of precursors and laser systems. The most important results from these studies are: (a) there exists a threshold laser fluence for the onset of laser doping, and this coincides with the silicon-melting threshold [12,13]; (b) the depth of the laser diffused layers increases linearly with the laser fluence [14,15]; (c) using a high number of repeated laser pulses leads to a rectangular doping profile, with the doping depth corresponding to the melting depth [12,15-18]; and (d) infinite doping sources can be realized using gaseous precursors [12,13,18,19], while deposited precursors mostly act as exhaustive sources, leading to a decrease of

*barhdadi@ictp.it

the maximum doping concentration upon multiple irradiation [16,17].

In spite of the vast scientific effort spent on characterizing the laser doping process at that time, and the first solar cells that were produced [14,20], no real development of laser doping for photovoltaic technology was reported until the beginning the 21st century, when the solar industry commenced its incredible growth, and the search for cheaper solar cell production processes intensified. At that time researchers started examining laser doping for full area silicon solar cell emitters [21-24], as well as selective emitters [25-27]. Several groups are also working on selective emitter formation from a phosphorous glass layer [28], from pre-deposited doping layers [29,30], or from a liquid doping containing jet [31].

The purpose of the present work is to analyze laser irradiated silicon materials without being doped at the same time. This approach allows for separating the effects of the laser process itself from the influence of employed doping precursors. The paper should be considered as a review of previous studies we already did and published on damage and other detrimental effects caused by lasers during semiconductors and solar cells processing [32-47]. Since research and developments on the use of lasers in new

photovoltaic technologies are experiencing a renewed interest, in part because of laser doping, we believe that it is worthwhile to re-examine in this review the issue of laser damage with updated interpretations and comments.

2. Laser Doping Process

The following section describes the laser doping process, using pre-deposited precursor layers as usually employed. The fundamental working principle is identical to most of the other known laser doping processes. The main difference lies in the application and structure of the doping precursor, which is performed prior to the process itself.

As schematically presented in Fig. 1, the semiconductor substrate we prepared to dope is mounted on an X-Y table. The top surface of this substrate is thereafter coated by the doping precursor layer deposited by a spin-coating procedure, or by sputtering or by electron-gun evaporation. The precursor layers are always directly in touch with the semiconductor substrate, without any inter-layers in between. A more detailed description of the complete process can be found in [1].

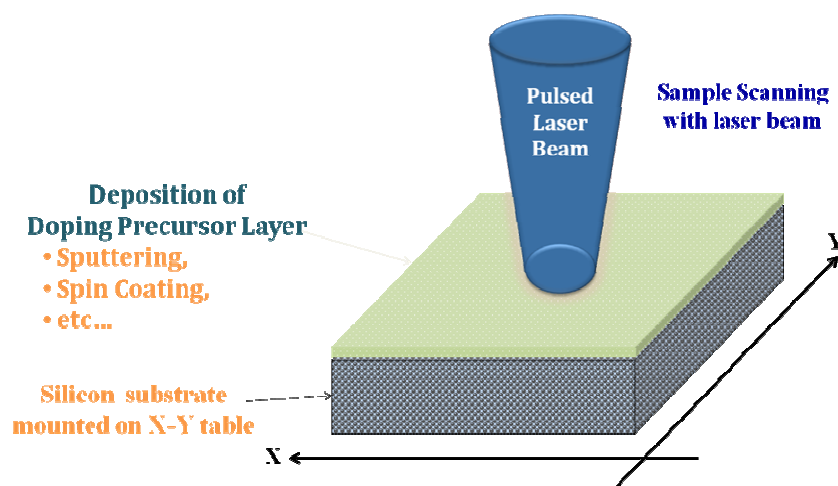


Fig.1: Laser doping process requirements and experimental procedure.

After the doping precursor layer deposition, the laser doping process itself starts by focalizing and scanning the entire coated surface by a pulsed laser beam. Based on the extensive research on laser melting and doping of semiconductors presented in

[1], as well as the experience gathered in the course of our team's previous work [32-47], the laser doping process is hypothesized to consist of the stages depicted in Fig. 2.

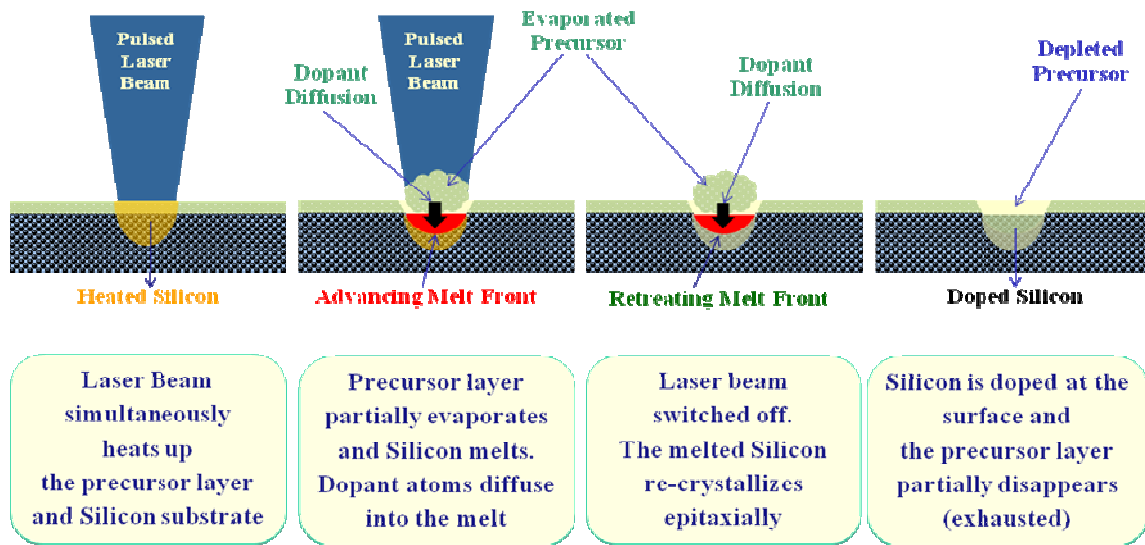


Fig.2: The laser process, employing pre-deposited dopant precursor layers, consists of several steps: a) The impinging laser pulse simultaneously heats up the precursor and the silicon; b) the precursor (partially) evaporates and the silicon melts. Dopant atoms diffuse into the melt; c) the laser pulse ceases and the melt front retreats. The liquid silicon re-crystallizes epitaxially; and d) a doped silicon layer remains at the surface. The precursor is either partially or completely exhausted.

First, the laser irradiation heats up the precursor layer and the underlying semiconductor substrate. Depending on the transparency of the doping precursor layer it is due to either direct light absorption or heat transfer from the underlying silicon. The precursor evaporates and forms a dense vapor phase above the illuminated area. Next, the irradiated surface of semiconductor substrate melts and the melt front advances into the bulk. As soon as the silicon is molten, a liquid state diffusion process of dopant atoms starts. When the energy supply from the laser pulse ceases the melt front reverses and the molten silicon re-crystallizes epitaxially. The remaining doped area is several 100 nm thick. The size of the doped area depends on the size of the laser focus on the surface of substrate. In order to process larger areas, single laser spots are placed next to one another by moving the sample on a X-Y table as shown and described in Fig. 1.

3. Experimental Procedure

The investigations were carried out on both n-type chemically etched and p-type pre-polished samples that were cut from 4 kinds of low resistivity, <100> oriented and virgin mono-crystalline silicon wafers, which are: (a) P-doped, float-zone (FZ), 1-5 $\Omega\cdot\text{cm}$; (b) P-doped, Czochralski (CZ), 1-5 $\Omega\cdot\text{cm}$; (c) P-doped, FZ, 2 $\Omega\cdot\text{cm}$; and (d) B-doped, pre-polished FZ, 10 $\Omega\cdot\text{cm}$. This diversity of samples allows us to look at the influence of the starting wafer on the

outcome. The samples were first degreased in boiling trichloroethylene for 5 min., cleaned in acetone, rinsed in running de-ionized water and dried with flowing nitrogen gas. Next, n-type (P-doped) samples were chemically etched in a CP₄ etching mixture (HNO₃:HF:CH₃COOH acids combination at 5:3:3 proportions) for 2 minutes. They were then carefully rinsed in dilute hydrofluoric acid (HF:H₂O) in equal proportions (1:1). Next, they were rinsed again in running de-ionized water and finally dried under nitrogen gas flux to be ready for laser irradiation treatments. The following processes were performed immediately after chemical preparation of the samples using three different types of lasers:

1) Using a solid-state Nd-YAG pulsed laser (from Quantronix, USA), operating at 530 nm wavelength λ . This laser delivers pulses of about 100 ns duration and a small spot diameter ($\varnothing = 0.1$ mm typically) but at a very high repetitive rate of up to 10 kHz. In this case, large areas are covered by scanning the pulsed beam under controlled overlapping conditions. The laser beam fluence E has been varied from 0.6 to 1.6 $\text{J}\cdot\text{cm}^{-2}$ (Table 1). As is published elsewhere [48], the silicon melt depth at 1.6 $\text{J}\cdot\text{cm}^{-2}$ for this pulsed laser is estimated to be about 500 Å.

2) Using a solid-state ruby pulsed laser ($\lambda = 694.3$ nm) operating in the mono-mode released working

regime giving a single spot of about 9 mm diameter and pulses of 20 ns duration. The laser beam fluence E has been ranged from 0.6 to 1.2 J.cm⁻² (Table 1). With this pulsed laser, it has been shown that silicon melt depth of about 500 Å is reached at a fluence $E = 1$ J.cm⁻² [48].

3) Using a gas-state ArF excimer pulsed laser (from Spectra Physics) operating in ultraviolet at $\lambda = 193$ nm. This laser processing was performed in air by adjusting laser pulses to 21 ns, focused to a size of 2 x 20 mm² and scanned on the sample in one direction by means of an X-Y stage. Prior to irradiation, a thermally grown oxide film of about 200 nm thickness was formed on the sample surface in order to limit the degradation since the presence of this film reduces the thermal quenching [49]. The laser fluence varied between 0.5 and 1 J.cm⁻² (Table 1), which is well above the melting threshold of crystalline silicon [50]. After laser irradiation, the oxide film was removed.

To analyze the samples, Schottky diodes were performed by evaporating aluminum/titanium or

gold dots of 1 to 1.2 mm diameter onto the p- or n-type laser exposed surfaces, respectively. On the back surfaces, Ohmic contacts were also performed by evaporation of aluminum or gold depending on the type of silicon sample. Schottky diodes were also formed on un-irradiated reference samples at the same time to be sure that what we observed was due to the laser irradiation. Next, current-voltage (I-V) and capacitance-voltage (C-V) characteristics of the diodes have been measured at room temperature and their most important electrical parameters have been deduced. Additional measurements at low temperature have also been performed. The induced active defects generated in the bulk of the samples were investigated by the deep level transient spectroscopy (DLTS) technique. The DLTS system used consists of a 1 MHz capacitance bridge and a double-phase lock-in detector method providing a square weighting function. The energy levels and the capture cross sections are determined using the emission Arrhenius plots.

Table 1: Nd-YAG, ruby and excimer pulsed laser processing experimental conditions.

	Pulsed Nd-YAG laser	Pulsed ruby laser	ArF pulsed excimer laser
Wave Length λ	530 nm	694.3 nm	193 nm
Pulse Duration	100 ns	20 ns	21 ns
Pulse Frequency	10 kHz (Very high repetitive rate)	1 - 5 Hz	10 Hz
Beam Spot Size	$\varnothing = 0.1$ mm	$\varnothing = 9$ mm	2 x 20 mm ²
Beam Fluence E	From 0.6 to 1.6 J.cm ⁻² (melting threshold = 1 J/cm ²)	From 0.6 to 1.2 J.cm ⁻² (melting threshold = 0.8 J.cm ⁻²)	From 0.5 to 1 J.cm ⁻² (melting threshold = 0.5 J.cm ⁻²)
Processing Temperature	Ambient	Ambient	Ambient

4. Experimental Results and Discussion

4.1. Samples processed with pulsed Nd-YAG laser

I-V characteristics of Schottky diodes made on Nd-YAG laser processed samples have been recorded as a function of the laser beam fluence E . Schottky diodes made on reference non irradiated samples exhibit good and reproducible rectifier electrical characteristics. For low fluences ($E \leq 0.9$ J.cm⁻²), the I-V behavior of a reference device remains well preserved. The rectifier effect disappears at nearly $E = 1$ J.cm⁻². When the fluence goes up, a drastic degradation occurs and the I-V curves become no longer rectifying indicating the formation of a quasi-Ohmic contact. It can be noticed that I-V

measurements performed at 77 K do not show the same experimental results. Indeed, in the case of samples irradiated at 1.3 J.cm⁻² the I-V curves show a quasi-Ohmic behavior at 300 K, but at 77 K they are very close to that of the reference Schottky diode.

Fig. 3 shows the evolution of the potential barrier height V_{bn} with the laser beam fluence E . V_{bn} has been calculated from the forward saturation current of Schottky diodes by assuming a pure thermionic transport. Starting from a typical value of 0.75 V for the reference diode, V_{bn} remains practically constant for the lower fluences ($E \leq 0.9$ J.cm⁻²). With increasing E , V_{bn} decreases slightly after 1 J.cm⁻² and goes down continuously

to reach very low values (< 0.6 V) for the higher fluences.

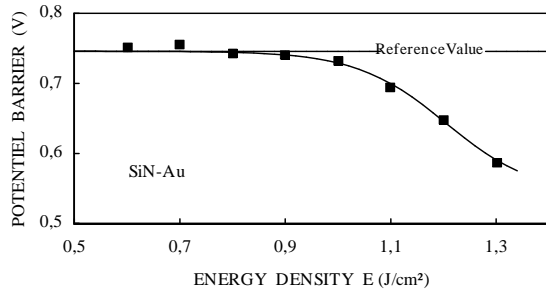


Fig.3: Evolution of the potential barrier height V_{bn} of Au-Si(N) Schottky diodes as a function of pulsed Nd-YAG laser fluence. A strong electrical degradation in V_{bn} occurs at ~ 1 J.cm⁻² threshold.

The change in the diode quality factor n as a function of laser fluence is reported in Fig. 4. Starting from a typical 1.15 value for the reference Schottky diode, n remains practically unchanged for the lower fluences. At nearly $E = 1$ J.cm⁻², n shows a small increase and then goes up continuously to reach values higher than 3 for $E > 1.3$ J.cm⁻².

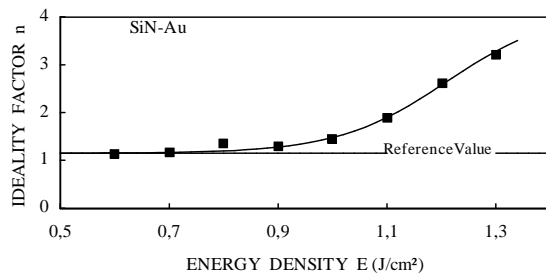


Fig.4: Evolution of the ideality factor n of Au-Si(N) Schottky diodes as a function of pulsed Nd-YAG laser fluence. A strong electrical degradation in n occurs at ~ 1 J.cm⁻² threshold.

Capacitance-Voltage measurements have been carried out at 1 MHz frequency. Fig. 5 shows the evolution of the diode capacity at -0.5 V with the laser beam fluence E . Lower fluences induce practically no change in the measured capacity. However, at $E = 1$ J.cm⁻² the capacity starts increasing significantly and quickly becomes very high for the higher fluences indicating an increased concentration of ionized donor centers close to the sample surface.

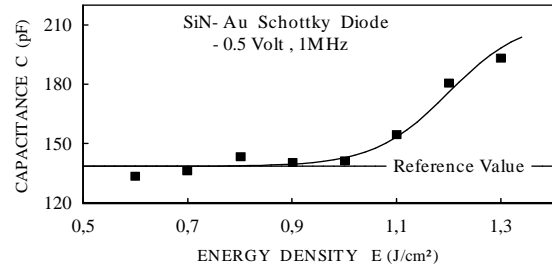


Fig.5: Evolution of the capacitance C measured at -0.5 V of Au-Si(N) Schottky diodes as a function of pulsed Nd-YAG laser fluence. A strong increase of C (-0.5 V) value occurs at ~ 1 J.cm⁻² threshold.

From the above results, we notice practically the same fluence threshold around 1 J.cm⁻² for which all the electrical properties of the diodes start to degrade. Indeed, for beam fluence lower than 1 J.cm⁻², Nd-YAG laser produces only very small changes in the diode electrical parameters. However, above this threshold a fast degradation occurs and all of the diode electrical properties indicate practically the same behavior and the coherent trends. The sharp increase of the capacity measured at -0.5 V, as well as the great difference observed between I-V curves recorded at 77 K and at 300 K, indicate that high concentration of donor centers are induced by laser irradiations in the vicinity of the processed sample surfaces. Computer simulations through a model calculation [51] have shown that, for fluence $E \geq 1$ J.cm⁻², the silicon processed layer turns into melt. So, we think that the most damaging defects responsible for the diode degradation are generated in the laser induced molten layer and we believe that they result from the quenching process due to the fast melt cooling and high solidification rate.

Fig. 6 shows a typical DLTS spectrum recorded from Au-Si(N) Schottky diode made on n-type Si sample irradiated with pulsed Nd-YAG laser at 1.6 J.cm⁻² fluence, which is well above the melting energy threshold (~ 1 J.cm⁻²). DLTS spectrum was recorded at emission rate of 14 s⁻¹ and pulse duration of 600 μ s. Three electron traps E_1 (0.32 eV) with $\sigma_{n1} = 8.10^{-16}$ cm², E_2 (0.45 eV) with $\sigma_{n2} = 2.10^{-16}$ cm², and E_3 (0.53 eV) with $\sigma_{n3} = 6.10^{-16}$ cm² are observed. As we will see in the next paragraph, these electron traps are also observed in the case n-type Si of low resistivity irradiated at 1 J.cm⁻² with ruby pulsed laser.

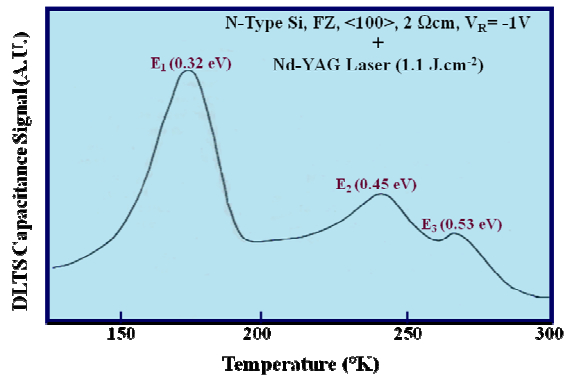


Fig.6: DLTS spectrum recorded from Au-Si(N) Schottky diode made on n-type Si sample irradiated with pulsed Nd-YAG laser at 1.6 J.cm^{-2} fluence, which is well above the melting energy threshold ($\sim 1 \text{ J.cm}^{-2}$). DLTS spectrum was recorded at emission rate of 14 s^{-1} and pulse duration of $600 \mu\text{s}$. One observes three electron traps: $E_1(0.32 \text{ eV})$ with $\sigma_{n1} = 8.10^{-16} \text{ cm}^2$, $E_2(0.45 \text{ eV})$ with $\sigma_{n2} = 2.10^{-16} \text{ cm}^2$, and $E_3(0.53 \text{ eV})$ with $\sigma_{n3} = 6.10^{-16} \text{ cm}^2$.

4.2. Devices processed with ruby pulsed laser

The experimental procedure and study described above has been entirely and systematically carried out again in exactly the same experimental conditions except that Nd-YAG laser has been substituted for Pulsed Ruby laser. The fluence threshold, for which a significant degradation in Schottky diode electrical characteristics and properties occurs, was about $0.7 - 0.8 \text{ J.cm}^{-2}$. This degradation threshold also coincides with the beam fluence for which the surface processed layer of the silicon sample turns into melt [51].

Fig. 7 shows a typical DLTS spectrum from Au-Si(N) Schottky diode performed on a ruby laser irradiated sample at 1 J.cm^{-2} fluence, which is above the melting and electrical degradation energy threshold ($\sim 0.8 \text{ J.cm}^{-2}$) [52]. The spectrum exhibits three main peaks labeled E_1 , E_2 and E_3 due to electron traps located respectively at 0.32 eV , 0.43 eV and 0.58 eV below the conduction band. The corresponding capture cross sections of the traps are $4.4 \cdot 10^{-16} \text{ cm}^2$, $1.4 \cdot 10^{-16} \text{ cm}^2$ and $5 \cdot 10^{-15} \text{ cm}^2$, respectively. The dominant defect peak in the spectrum, i.e., the $E_c-0.32 \text{ eV}$ trap, gave a concentration of about $6 \cdot 10^{14} \text{ cm}^{-3}$ at -1 V reverse bias and 50 s^{-1} emission rate.

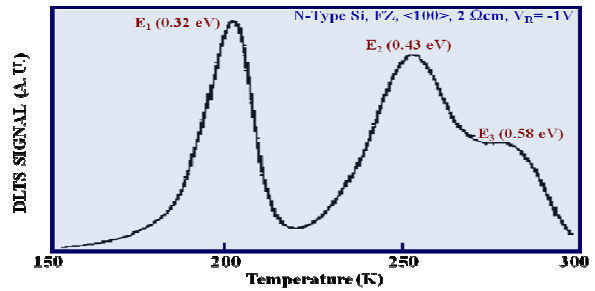


Fig.7. DLTS spectrum from Au-Si(N) Schottky diode after pulsed ruby laser at 1 J.cm^{-2} beam fluence which is above the melting energy threshold. The spectrum exhibits three main peaks labeled E_1 , E_2 and E_3 due to electron traps located respectively at 0.32 eV , 0.43 eV and 0.58 eV below the conduction band.

These deep levels are similar to those observed above in the case of silicon samples irradiated with pulsed Nd-YAG laser with beam fluence of 1.6 J.cm^{-2} , which is well above the melting and electrical degradation threshold [53]. Considering the fact that the melt depths induced in the silicon wafers by the two lasers at their corresponding energies (1 J.cm^{-2} for ruby and 1.6 J.cm^{-2} for Nd-YAG) are approximately equal ($\sim 500 \text{ \AA}$) [51], it is not surprising that the same levels are observed here. This suggests that the essential parameters in defect formation during liquid-phase processing is the melt depth and the velocity of solidification or melt cooling rate. A situation in which melt depths are equal and natural cooling is employed produces the same defects irrespective of the type of laser used. This happens to be the case in our experiments. The defect states produced are characteristics of pulsed laser-treated silicon for which some tentative identification methods were proposed [32, 54, and 55]. In our previous works, we have showed that these defects can be electrically neutralized either by low-energy hydrogen ion implantation [39] or by rapid thermal annealing at 600°C for 60 s duration [53].

From the analyses and comparison of DLTS spectra obtained on samples irradiated separately by Nd-YAG and ruby lasers (Table 2), one can conclude that active defects induced in silicon by these two solid-state pulsed lasers are similar.

Table 2: Similarity of defects deep levels induced by the two solid-state Nd-YAG and Ruby pulsed lasers.

Solid State Pulsed Laser	Deep Level E ₁	Deep Level E ₂	Deep Level E ₃
Nd-Yag	E _C - 0.32 eV σ _n ~ 8.10 ⁻¹⁶ cm ⁻²	E _C - 0.45 eV σ _n ~ 2.10 ⁻¹⁶ cm ⁻²	E _C - 0.53 eV σ _n ~ 6.10 ⁻¹⁶ cm ⁻²
Ruby	E _C - 0.32 eV σ _n ~ 4.4 10 ⁻¹⁶ cm ⁻²	E _C - 0.43 eV σ _n ~ 1.4 10 ⁻¹⁶ cm ⁻²	E _C - 0.58 eV σ _n ~ 5 10 ⁻¹⁵ cm ⁻²

4.3. Devices processed with ArF excimer pulsed laser

Figs. 8 and 9 show typical DLTS spectra of deep levels observed in p-type silicon irradiated with ArF excimer laser at fluences of 0.55 J.cm⁻² and 0.7 J.cm⁻², respectively. The DLTS spectrum of an un-annealed (control) sample is also reported for comparison. Four hole traps H₁ (≈ 0.22 eV), H₂ (0.37 eV), H₃ (0.48 eV), and H₄ (0.6 eV) are detected on the irradiated sample at an emission rate of 41 s⁻¹ and using a pulse width of 120 μs. The capture cross sections σ_p are 3 10⁻¹⁶ cm², 1 10⁻¹⁵ cm² and 3 10⁻¹⁴ cm² for H₂, H₃ and H₄, respectively. For p-type material, there is, to our knowledge, only the previously mentioned result of Young et al. [56] probably due to difficulties in performing good Schottky diodes on p-type silicon. A comparison of the H₂ level with the single level observed at Ev + 0.38 eV in this work shows good match. However, this analysis was performed on Schottky structures made on Si-implanted p-type Si after XeCl annealing at 2 J.cm⁻². We believe that their level is due to a residual tail of implanted defects which subsist in a region deeper than the molten layer. A trap at Ev + 0.38 eV has often been observed on N-P junctions prepared by ion bombardment with subsequent laser annealing [32,57,58].

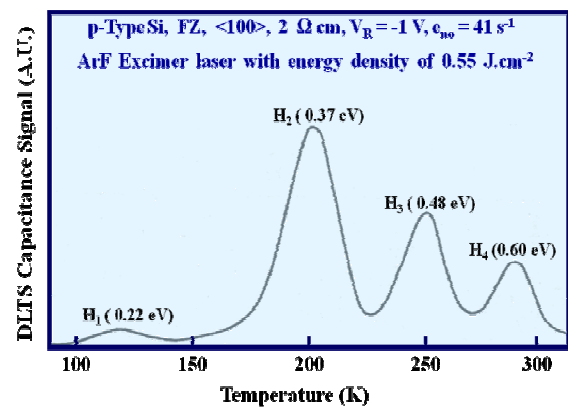


Fig.8: DLTS spectrum recorded on p-type silicon sample irradiated with ArF excimer laser at fluence of 0.55 J.cm⁻².

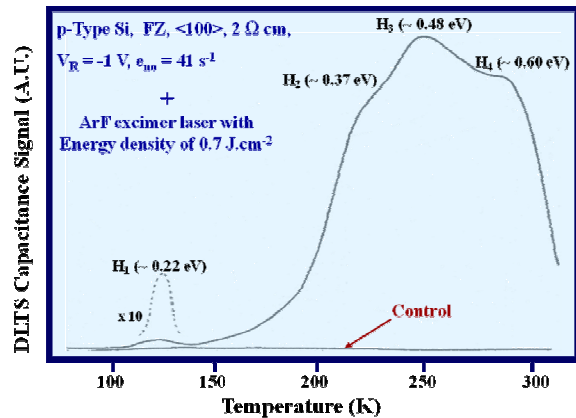


Fig.9: DLTS spectra recorded on irradiated and un-irradiated (control) p-type silicon samples. The ArF excimer laser fluence is 0.7 J.cm⁻². The H₁ level is amplified by 10 to be well detected.

The H₁, H₂, and H₃ levels have also been seen in p-type Si irradiated with solid state lasers [59,60]. These results are not surprising since it is known that the essential parameters in the defect formation during liquid-phase processing are the

melt depth and the velocity of solidification or melt cooling rate. In a situation when melt depths are equal and natural cooling is employed, it produces the same defects regardless of the laser type. However, in the case of excimer laser irradiation, an additional trap (H_4) located at about 0.6 eV from the valence band is observed whose origin is not clear and needs more investigation. If the quenching model is considered, where the vacancies generated at high temperature could precipitate during the fast cooling, it is possible to relate the observed defects to vacancy clusters or vacancy-impurity associations. Thus, the H_1 trap has been correlated with the lowest energy charge state of the di-vacancy, while H_2 and H_3 have been assigned to the vacancy-oxygen-carbon (V-O-C) complex and to the vacancy-boron (V-B) complex [60], respectively.

A typical DLTS spectrum (curves 1 and 2) for ArF laser irradiated n-type silicon sample is shown in Fig. 10. The DLTS spectrum for the reference sample is also reported in the same figure for comparison (curve 3). Six electron traps are clearly detected and correlated to the laser induced defects: the peaks are E_1 (~ 0.18 eV), E_2 (~ 0.25 eV), E_3 (0.34 eV), E_4 (0.43 eV), E_5 (0.53 eV) and E_6 (0.60 eV). The capture cross section σ_n corresponding to these traps are 5.10^{-16} cm², 1.10^{-15} cm², 1.10^{-15} cm² and 5.10^{-14} cm² for E_3 , E_4 , E_5 and E_6 , respectively. The de-convolution of the peaks has been performed by changing the pulse excitation amplitude as shown by curve 2. The defects E_1 - E_6 have been previously observed by many authors for solid state laser annealing of virgin silicon [32]. The corresponding energies coincide within 0.04 eV with those found for ruby lasers [32,33,57,61,62,63] and within 0.02 eV for Nd-YAG lasers [34,55,63].

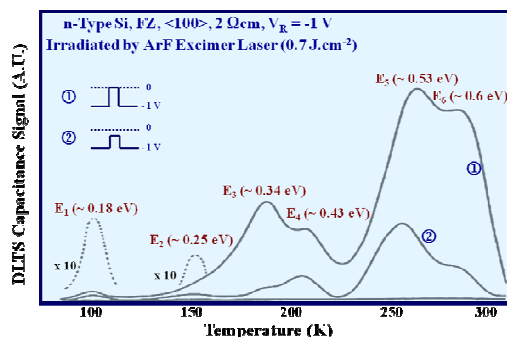


Fig.10: DLTS spectra recorded on irradiated (curves 1 and 2) and un-irradiated (curve 3), n-type silicon samples. Curve 2 is obtained by changing the pulse excitation amplitude. The E_1 and E_2 traps are amplified by 10 to be well observed.

The E_1 (0.18 eV) and E_2 (0.25 eV) defects are detected in a very low concentration under our experimental conditions. The origin of the E_1 peak is subject to discussion. It is thought to be due either to in-diffusion of an impurity from the surface [55,62] or to a quenched-in defect resulting from re-crystallization from the liquid phase [32,55,62]. The trap E_2 (0.25 eV) has been correlated to the di-vacancy (V-V) defect. The trap at $E_c - 0.34$ eV can probably be assigned to a multi-vacancy center [55]. The deeper levels E_4 and E_5 have generally been associated with di-vacancy (0.43 eV) [63] and the vacancy-oxygen complex or clusters of vacancy like surface defects (0.53 eV) [58,64]. This last level seems to be a recombination center as it was also detected as minority carrier trap in a MCTS [32] measurement. This is probably the case for our H_4 and E_6 levels which appear in both silicon types. More investigations are necessary to confirm this point.

Depth profiles of the traps E_3 , E_4 , E_5 and E_6 after ArF excimer laser irradiation at fluence of 0.7 J.cm⁻² have also been determined [36]. It is obvious that the traps are present in the silicon surface at a region deeper than the melt depth (about 100 nm at 0.7 J.cm⁻²) [65]. The concentration of the levels falls quickly under the detection limit for depths greater than 1 μ m. Moreover, the defect distribution decreases strongly following an exponential trend. The extrapolation towards the surface can give very large defect concentrations which might explain the difficulties in forming rectifying contacts on this damaged surface. We have also shown that a post laser thermal treatment around 650°C allows most of these defects [66] to anneal out. This result enhances the interest of the excimer laser applications in silicon processing.

5. Conclusion

In summary, this work has clearly demonstrated that all pulsed lasers considered generate electrically active defects in silicon. These defects are generated for fluences above the melting threshold value which is depending on the type of laser. Defects are mostly generated in the laser induced molten layer, and are concentrated in the vicinity of the surface. So, we believe that the generated defects are resulting from the quenching process due to the fast melt cooling and immediate fast re-solidification of the irradiated silicon layer. The active defects induced by solid-state pulsed lasers (Nd-YAG and ruby) are similar to those generated by gas-state ArF excimer laser, so the electrically active defects resulting from all pulsed

lasers working in the liquid phase regime seem to be solely related to the re-growth velocity as was speculated in the past. Generated defects are acting either as charge carrier traps or as recombination centres. This is why they have negative effect on the electrical performances of solar cells.

References

- [1] M. F. Ametowobla, Dr. Ing. Thesis, Institut für Physikalische Elektronik der Universität, Stuttgart, Germany, 2010.
- [2] Y. Nishihara, Y. Takahashi, A. Ogane, J. Nigo, Y. Uraoka and T. Fuyuki, Proceedings of the 21th EU-PVSEC, Dresden (2006) p.941.
- [3] T. Akane, T. Nii and S. Matumoto, Jpn. J. Appl. Phys. **31**, 4437 (1992).
- [4] C. White, S. Wilson, B. Appleton and F. Young, J. Appl. Phys. **51**, 738 (1980).
- [5] C. White, *Pulsed Laser Processing of Semiconductors*, Eds. R. Beer and C. Albert (Academic Press, N.Y., 1984).
- [6] C. White, P. Pronko, S. Wilson, B. Appleton, J. Narayan and R. Young, J. Appl. Phys. **50**, 3261 (1979).
- [7] R. Wood and G. Giles, Phys. Rev. **B23**, 2923 (1981).
- [8] R. Wood, J. Kirkpatrick and G. Giles, Phys. Rev. **B23**, 5555 (1981).
- [9] R. Wood, Phys. Rev. **B25**, 2786 (1982).
- [10] R. Wood, C. White and F. Young, *Semiconductors and Semimetals*, Vol.23, Eds. R. Beer and C. Albert (Academic Press, New York, 1984).
- [11] J. Poate and J. Mayer, *Laser Annealing of Semiconductors* (Academic Press, 1982).
- [12] D. Debarre, K.G.T. Noguchi and J. Boulmer, IEICE Trans. Electron. E85-C, 1098 (2002).
- [13] T. Deutsch, D. Ehrlich, D. Rathman, D. Silversmith and R. Osgood, J. Appl. Phys. Lett. **39**, 825 (1981).
- [14] E. Fogarassy, R. Stuck, J. Grob and P. Siffert, J. Appl. Phys. **52**, 1076 (1981).
- [15] Y. Wong, X. Yang, P. Chan and K. Tong, Appl. Surf. Sci. **64**, 259 (1993).
- [16] E. Fogarassy, D. Lowndes, J. Narayan and C. White, J. Appl. Phys. **58**, 2167 (1985).
- [17] D. Bollmann, G. Neumayer, R. Buchner and K. Habberger, Appl. Surf. Sci. **69**, 249 (1993).
- [18] G. Kerrien, J. Boulmer, D. Debarre, D. Bouchier, A. Grouillet and D. Lenoble, Appl. Surf. Sci. **186**, 45 (2002).
- [19] G. Bentini, M. Bianconi, L. Correa, R. Nipoti, D. Patti and A. Gasparotto, Appl. Surf. Sci. **36**, 394 (1989).
- [20] T. Deutsch, J. Fan, G. Turner, R. Chapman, D. Ehrlich and R. Osgood, J. Appl. Phys. Lett. **38**, 144 (1981).
- [21] A. Esturo-Breton, J. Kohler and J. Werner, Proc. 13th Workshop on Crystalline Silicon Solar Cell Materials and Processes (NREL, Golden, Colorado, USA, 2003) p.186.
- [22] A. Esturo-Breton, M. Ametowobla, C. Carlsson, J. Kohler and J. Werner, Proc. 21st European Photovoltaic Solar Energy Conference, Eds. H. Palz, H. Ossenbrink and P. Helm (WIP Munich, 2006) p.1247.
- [23] M. Ametowobla, A. Esturo-Breton, J. Kohler and J. Werner, Proc. 31st IEEE Photovolt. Spec. Conf. (IEEE, Piscataway, 2005) p.1277.
- [24] M. Ametowobla, J. Kohler, A. Esturo-Breton and J. Werner, Proc. 22nd European Photovoltaic Solar Energy Conference, Eds. W. Palz and H. Ossenbrink (WIP Munich, 2007) p.1403.
- [25] T. Roder, P. Grabitz, S. Eisele, C. Carlsson, J. Kohler and J. Werner, Proc. 34th IEEE Photovolt. Spec. Conf. (IEEE, Piscataway, 2009).
- [26] C. Carlsson, A. Esturo-Breton, M. Ametowobla, J. Kohler and J. Werner, Proc. 21st European Photovoltaic Solar Energy Conference, Eds. W. Palz and H. Ossenbrink (WIP Munich, Germany, 2006) p.938.
- [27] J. Carlsson, C. Kohler and J. Werner, Proc. 17th IEEE Photovolt. Spec. Conf. (IEEE, Piscataway, 2007) p.538.
- [28] <http://www.ipe.uni-stuttgart.de/>
- [29] B. Tjahjono, J. Guo and Z. Hameiri, Proc. 22nd European Photovoltaic Solar Energy Conference, Eds. W. Palz and H. Ossenbrink (WIP Munich, Germany, 2007) p.966.
- [30] B. Tjahjono, S. Wang and A. Sugianto, Proc. 23rd European Photovoltaic Solar Energy Conference, Eds. W. Palz and H. Ossenbrink (WIP Munich, Germany, 2008) p.1995.
- [31] D. Kray, A. Fell, S. Hopmann, K. Mayer, M. Mesec, S. Glunz and G. Willeke, Proc. 22nd European Photovoltaic Solar Energy Conf., Eds. W. Palz and H. Ossenbrink (WIP Munich, Germany, 2007) p.1227.
- [32] A. Mesli, J. C. Muller and P. Siffert, Laser Solid Interactions and Transient Thermal Processing of Materials, Suppl. of J. de Phys., **C44**, No.5, 281 (1983).
- [33] A. Slaoui, A. Barhdadi, J-C. Muller and P. Siffert, Appl. Phys. **A39**, 159 (1986).
- [34] W. O. Adekoya, J. C. Muller and P. Siffert, Appl. Phys. Lett. **49**, No.21, 1429 (1986).

- [35] W. O. Adekoya, Ph.D. Thesis, University of Paris VII (1987), France.
- [36] B. Hartiti, A. Slaoui, J. C. Muller and P. Siffert, *J. of Appl. Phys.* **66**, No.8, 3934 (1989).
- [37] B. Hartiti, A. Slaoui, J. C. Muller and P. Siffert, *Materials Science and Eng. B* **4**, Nos.1-4, 257 (1989).
- [38] B. Hartiti, A. Slaoui, J. C. Muller and P. Siffert, *Appl. Surf. Sci.* **46**, Nos.1-4, 371 (1990).
- [39] B. Hartiti, Ph.D. Thesis, University Louis Pasteur I, Strasbourg 1990, France.
- [40] A. Barhdadi, H. Amzil, N. M'gafad, J. C. Muller and P. Siffert, *Proceedings of the First International Workshop on the Physics and Modern Applications of Lasers*, 22-28 May 1991, Dakar, Senegal, p.359.
- [41] A. Barhdadi, *Deuxième Ecole Euro-Maghrébine MEDISOL'2*, 19-25 Sept. 1995, Marrakech, Morocco.
- [42] A. Barhdadi and J. C. Muller, *Fourth International Workshop on the Physics and Modern Applications of Lasers*, 6-14 Jan. 1996, Khartoum, Sudan.
- [43] A. Barhdadi and J. C. Muller, *Revue des Energies Renouvelables* **3**, No.1, 29 (2000).
- [44] A. Barhdadi and J. C. Muller, *Proceedings of the "Deuxièmes Journées d'Optique"*, 27-28 April 2000, Meknes, Morocco, p.82.
- [45] A. Barhdadi and B. Hartiti, *International Conference on Optics and Lasers in Science and Technology for Sustainable Development* 11-16 Jan. 2010, University Cheikh Anta Diop, Dakar, Senegal.
- [46] A. Barhdadi, B. Hartiti and J. C. Muller, *International Workshop on Optics and Photonics*, 5-8 Oct. 2010, Cadi Ayyad University Marrakech, Morocco.
- [47] A. Barhdadi and B. Hartiti, *2nd International Conference in Laser Science and its Applications* 7-9 Dec. 2010, Khartoum, Sudan.
- [48] J. C. Muller, *State doctorate thesis*, Louis Pasteur University, Strasbourg, France, 1982.
- [49] T. Heiser, A. Mesli. E. Courcelle and P. Siffert, *J. Appl. Phys.* **64**, 4031 (1988).
- [50] F. Foulon, E. Fogarassy, A. Slaoui, C. Fuchs, S. Unamuno and P. Siffert, *Appl. Phys.* **A45**, 361 (1988).
- [51] M. Toulemonde and P. Siffert, *Appl. Phys.* **25**, 139 (1981).
- [52] D. Barbier, M. Remram, J. F. Joly and A. Laugier, *J. Appl. Phys.* **61**, 156 (1987).
- [53] W. O. Adekoya, J. C. Muller and P. Siffert, *Appl. Phys.* **A42**, 227 (1987).
- [54] Y. N. Nikiforov and V. A. Yanushkevich, *Sov. Phys. Semicond.* **14**, 314 (1980).
- [55] L. C. Kimerling and J. L. Benton, *Laser and Electron Beam Processing of Material*, Eds. C. W. White and P. S. Peercy (Academic, New York, 1980) p.385.
- [56] R. T. Young, J. Narayan, W. H. Christie, G. A. Van der Leaden, J. I. Levatter and L. J. Cheng., *Solid State Technol.* **26**, 183 (1983).
- [57] A. Mesli, J. C. Muller, D. Salles and P. Siffert., *Appl. Phys. Lett.* **39**, 159 (1981).
- [58] A. Mesli, A. Goltzene, J. C. Muller. B. Meyer, C. Schwab and P. Siffert, *MRS Symp. Proc.*, **4**, 349 (1982).
- [59] E. M. Lawson and S. J. Pearton, *Phys. Status Solidi* **A12**, K155 (1982).
- [60] K. L. Wang, Y. S. Lin, G. E. Passin, J. Karins and J. Corbett, *J. Appl. Phys.* **54**, 3839 (1983).
- [61] J. L. Benton, L. C. Kimerling, G. L. Miller, D. A. Robinson and G. K. Celler, *Laser-Solid Interactions and Laser Processing*, Eds. S. D. Ferris, H. J. Leamy, and J. M. Poate (American Institute of Physics, N.Y., 1978) p.543.
- [62] J. L. Benton, C. J. Doherty, S. D. Ferris, D. L. Flamm, L. C. Kimerling and H. J. Leamy, *Appl. Phys. Lett.* **36**, 670 (1980).
- [63] G. A. Kachurin, E. V. Nidaev, and N. V. Danyushkina, *Sov. Phys. Semicond.* **14**, 386 (1980).
- [64] Z. K. Fan, V. Q. Ho and T. Sugano, *Appl. Phys. Lett.* **40**, 418 (1982).
- [65] S. Unamuno and E. Fogarassy, *Appl. Surf. Sci.* **36**, 1 (1989).
- [66] E. Hartiti, A. Slaoui. J. C. Muller and P. Siffert, *Science and Technology of Defects in Silicon*, E-MRS Proceedings Symposium B, Eds. C. A. J. Ammerlaan and A. Chantre (North-Holland, N.Y., 1989).

Received: 18 October, 2011

Accepted: 20 October, 2011